



Subsurface-Controlled CO₂ Selectivity of PdZn Near-Surface Alloys in H₂ Generation by Methanol Steam Reforming

C. Rameshan⁴, W. Stadlmayr¹, C. Weilach², S. Penner¹, H. Lorenz¹, M. Hävecker⁴, R. Blume⁴,
T. Rocha⁴, D. Teschner⁴, A. Knop-Gericke⁴, R. Schlögl⁴, N. Memmel¹, D. Zemlyanov³,
G. Rupprechter², B. Klötzer¹

¹Institute of Physical Chemistry, University of Innsbruck, Innrain 52 A, 6020 Innsbruck (Austria)

²Institute of Materials Chemistry, Vienna University of Technology, Veterinärplatz 1, 1210 Vienna (Austria)

³Birck Nanotechnology Center, Purdue University, 1205 West State Street, West Lafayette, IN 47907-2057 (USA)

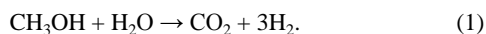
⁴Department of Inorganic Chemistry, Fritz-Haber-Institute of the Max-Planck-Society, Faradayweg 4–6,
14195 Berlin (Germany)

* Corresponding author: e-mail Bernhard.Kloetzer@uibk.ac.at,

Received: October 16, 2009, revised: November 24, 2009, published online: March 29, 2010

Keywords: heterogeneous catalysis · methanol steam reforming PdZn alloy · surface chemistry · water activation

For the use of polymer electrolyte membrane fuel cells (PEMFC) in future electric power generation, an efficient source of clean hydrogen is needed. In an effort of avoiding technical and safety problems of hydrogen handling, storage and transport, methanol can be used as practical and abundant energy carrier for stationary or on-board H₂ generation, as CH₃OH also has the advantage of higher energy density. Hydrogen generation from methanol can be performed by catalytic methanol steam reforming (MSR) [Eq. (1)].



This reaction must be carried out with high selectivity, avoiding the undesired by-product carbon monoxide which poisons the fuel cell electrocatalyst. A number of selective MSR catalysts are available. Apart from the classical Cu/ZnO catalyst, reduced states of Pd/ZnO, Pd/Ga₂O₃ or Pd/In₂O₃ have been identified as promising candidates [1]. The active phases in these catalysts are, however, alloys/intermetallics of PdZn, PdGa and PdIn, due to the partial reduction of the oxide support and subsequent alloying of Pd during reductive catalyst activation (on inert supports pure Pd produces only CO and H₂). In particular the

PdZn/ZnO catalyst combines the advantages of excellent catalytic selectivity and thermal stability [2]. However, the selectivity strongly depends on the exact experimental parameters of catalyst synthesis, oxidative and reductive gas treatments, annealing and reaction conditions. Furthermore, catalyst structure and composition typically change in the course of a catalytic reaction. Altogether, this makes establishing structure-selectivity correlations on technical catalysts very difficult and it is often unknown why two marginally different treatments of the same catalyst lead to very different selectivities.

Using a model catalyst approach of ultrahigh-vacuum (UHV) prepared PdZn surface alloys, combined with a detailed spectroscopic analysis of alloy structure, composition and catalytic activity both under UHV and under *in situ* conditions at mbar gas pressure, we show that the sensitive CO₂-selectivity of a PdZn 1:1 surface alloy is governed by the subsurface layer(s). Whereas a “multilayer” (≈5 layers) PdZn 1:1 near-surface alloy exhibits high CO₂-selectivity, a predominantly Pd-coordinated “monolayer” PdZn 1:1 surface, despite its virtually identical surface composition, only produces CO and H₂. This is explained by differences in the electronic and geometric structure of the two alloy surfaces, as monitored by

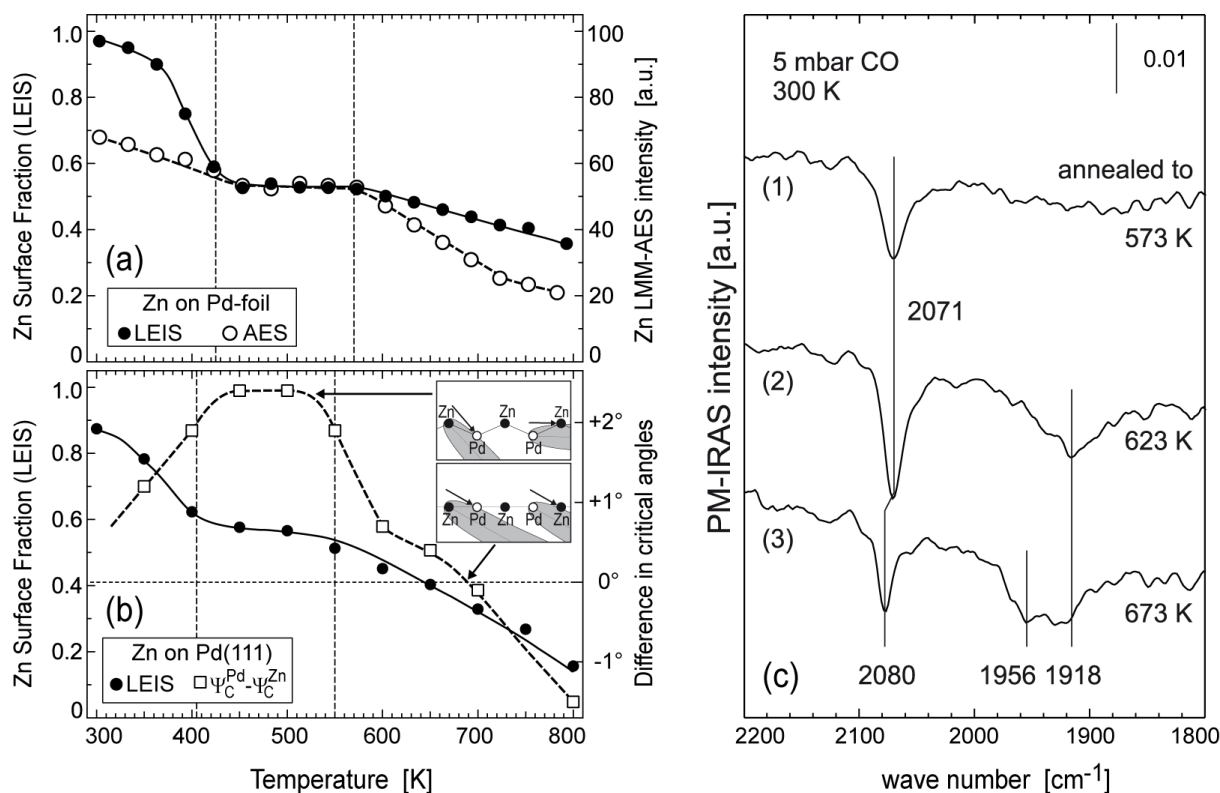


Fig. 1: (a): Pd:Zn surface fractions derived from LEIS and peak-to-peak intensity of the differentiated Zn-L3M45M45 (1G) Auger peak as a function of the annealing temperature. Initial Zn exposure was 3 ML at ≈ 300 K on Pd foil.

Fig. 1 (b): Filled circles: Pd:Zn surface fractions derived from LEIS for Zn films deposited on single crystal Pd(111) (Adapted from Ref. [7], note the close similarity to the LEIS data for Zn on Pd-foil in (a)). Open squares: Difference in critical angles for backscattering of 5 keV Ne ions from Pd and Zn atoms, respectively. In the schematic side views a corrugated and a non-corrugated (2x1) PdZn surface are depicted. Arrows and grey shadow cones indicate the critical angles where backscattering from Pd and Zn atoms, respectively, sets in. For illustration purposes the corrugation is largely exaggerated.

Fig. 1 (c): (1) PM-IRAS spectroscopy of CO adsorbed on the 1:1 PdZn multilayer alloy at 5 mbar and 300 K. Traces (2) and (3) are taken after annealing to 623 and 673 K, respectively.

synchrotron-based *in-situ* ambient pressure X-ray photoemission spectroscopy (AP-XPS), low-energy ion scattering (LEIS, ICISS), Auger electron spectroscopy (AES), polarization-modulated infrared reflection absorption spectroscopy (PM-IRAS), and kinetic tests in an all-glass reaction cell capable of operating between 10^{-10} and 1000 mbar. The results demonstrate the pronounced influence of the subsurface composition on the electronic and the geometric structures of the surface layer, which in turn governs the unique bifunctional catalytic action of the PdZn multilayer alloy: The predominant transformation of methanol to formaldehyde and the activation of water as Zn-OH species.

PdZn (near-)surface alloys grown by Zn deposition in ultrahigh vacuum on Pd(111) have been examined by a number of groups during the last years [3-7]. The focus was on the dependence of structure and composition on Zn coverage and deposition/annealing temperature. Based on previous studies and work presented herein, a procedure was developed to prepare distinct PdZn 1:1 alloy surfaces on Pd substrates, which are only different with respect to their Pd:Zn subsurface composition. For simplicity we denoted

them as “multilayer” and “monolayer” alloy states. Both exhibit a p(2x1) structure (1:1 PdZn surface ratio) on Pd(111), as verified by electron diffraction (LEED) (cf. Scheme 1, left).

The multilayer PdZn 1:1 surface alloy was prepared by evaporating an equivalent of 2-3 monolayers (ML) of Zn onto Pd(111) or Pd foil at 300 K (or below), followed by thermal annealing in vacuum at ≈ 500 K for 5-10 min. The LEIS data in Fig. 1 (b) indicate an invariant PdZn 1:1 surface composition for annealing temperatures between ≈ 430 and 570 K. This stability window is also corroborated by the AES data of Zn on Pd foil in Fig. 1 (a). XPS depth profiling (varying the kinetic energy of the photoelectrons between 100 eV and 900 eV; see supporting information S1) revealed that the multilayer alloy state exhibits a constant Pd/Zn composition for depths down to ≈ 5 monolayers.

The monolayer PdZn 1:1 surface alloy was obtained by Zn deposition (again 2-3 ML) at 300 K (or below), followed by thermal annealing in UHV at ≈ 630 K for 5-10 min. Whereas the surface composition remains close to 1:1,

as evident from LEIS, AES indicates that the Zn concentration in subsurface layers is considerably decreased (Fig. 1 (a)). The data depicted in Fig. 1 (a) were obtained for Zn deposited on Pd foil. Except for a small temperature shift of the stability regime by about 20K they correspond quite closely to LEIS experiments obtained for Zn films on single-crystal Pd(111) (Fig. 1 (b)). Obviously both types of substrates behave rather similar, as we could additionally corroborate by comparing the Pd3d core level and valence band spectra obtained both on Pd(111) and Pd foil during thermal annealing of 3 ML Zn (deposited at 300 K) between 440 K and 780 K in ultrahigh vacuum (see supporting information S2). The characteristic spectral changes from a Zn-rich to a Zn-lean chemical environment of Pd (compare 500 K “multilayer” and 630 K “monolayer” spectra in Fig. S2) were hardly different, i.e. at the same annealing temperature basically the same spectra were obtained on both substrates.

The altered subsurface composition induces an altered atomic geometry (viz. corrugation) of the surface layer as revealed by impact-collision ion scattering spectroscopy (ICISS). As shown in Fig. 1 (b), for the 500K multilayer state the critical angle Ψ_C^{Zn} for backscattering from Zn is by ≈ 2.5 degrees lower than Ψ_C^{Pd} for Pd atoms (details of ICISS scattering geometry and of definition of critical angle are given in the supporting information, experimental section). This indicates a corrugated surface with Zn atoms residing approx. 0.25\AA above their Pd counterparts. In contrast, after annealing to temperatures of 630K or above, the difference in critical angles is close to zero or negative, implying that the surface corrugation vanishes or even becomes inverted. This finding is in full agreement with DFT-calculations for Zn films on Pd(111), which predict a ‘Zn-up/Pd-down’ structure for 2 ML films, but ‘Zn-down/Pd-up’ for 1ML thick films [8].

The homogeneity of the 1:1 PdZn surface layer was examined by PM-IRAS spectroscopy using CO as probe molecule. Fig. 1 (c), trace (1) shows a spectrum of 5 mbar CO at 300 K, exhibiting a single sharp peak at 2070 cm^{-1} , characteristic of CO adsorbed on-top of individual Pd atoms. This proves the structural homogeneity of the multilayer alloy surface, because in case of remaining Pd patches hollow-bonded CO (at $\approx 1900\text{ cm}^{-1}$), bridge-bonded CO (at $\approx 1950\text{ cm}^{-1}$) and on-top CO (with coverage-dependent on-top CO frequencies from 2085 to $\approx 2100\text{ cm}^{-1}$) should additionally occur [9]. The vibrational frequency agrees very well with the on-top CO peak observed for PdZn-ZnO powder catalysts [10]. The $\approx -25\text{ cm}^{-1}$ wavenumber difference between on-top CO on Pd(111) and PdZn is due to a DFT-predicted charge transfer from Zn to Pd [11], enabling better backbonding which increases the on-top CO adsorption energy but weakens the internal C-O bond, thus leading to lower wavenumbers, as again predicted by DFT [8].

The lower spectra in Fig. 1 (c) show the effect of higher annealing temperatures. The 623K monolayer Zn-lean surface alloy additionally exhibits bridging CO at

$\approx 1920\text{ cm}^{-1}$, again in agreement with DFT [8]. The intensity increase of the on-top species is likely due to changes of surface corrugation, as discussed before. Higher annealing temperatures lead to spectra increasingly more similar to those of CO/Pd(111).

Since the multi- and monolayer alloy states are only distinct with respect to subsurface PdZn coordination geometry and –number, they represent the ideal test case for the electronic “ligand effect” likely influencing catalytic selectivity. Consequently, our in-situ spectroscopic approach was dedicated to potential differences of catalytic MSR selectivity under realistic reaction conditions close to technical catalysis.

The MSR activity/selectivity of the multilayer and monolayer alloys was comparatively studied by temperature-programmed reaction in the UHV-compatible high pressure cell operated as recirculating batch reactor at 1 bar. Fig. 2 (upper panel) reveals that the multilayer PdZn 1:1 surface alloy converts CH₃OH and water to CO₂ and formaldehyde CH₂O up to a temperature of 573 K, which is the upper limit of the multilayer stability. At temperatures above 573 K, CH₂O is consumed (cf. negative formation rate) and converted to CO via dehydrogenation, due to the progressive transformation toward the monolayer alloy at these temperatures. This was corroborated by performing the same reaction on the monolayer PdZn 1:1 surface alloy (Zn deposition at 300 K, followed by annealing to 630 K), which – similar to the pure Pd substrate – exhibited no

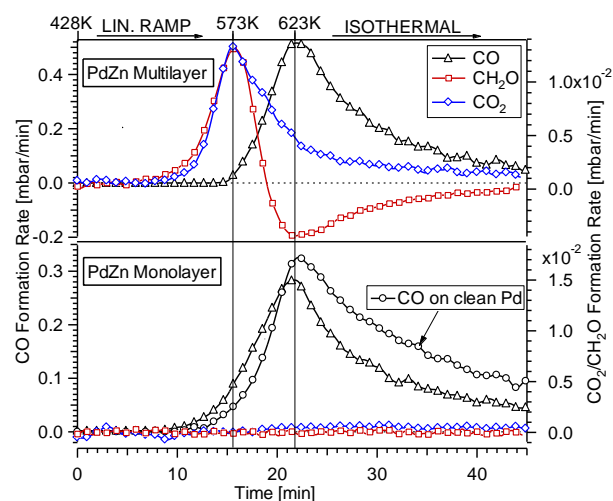


Fig. 2: Temperature-programmed methanol steam reforming on the multilayer PdZn 1:1 alloy on Pd foil (upper panel) versus MSR reaction on “Zn-lean” monolayer PdZn surface and MSR reaction on clean Pd foil (lower panel). Reaction conditions: 12 mbar methanol, 24 mbar water, 977 mbar He; linear temperature ramp (9.0 K/min) up to 623K, followed by isothermal reaction for 24 min. The decrease of the CO formation rate in the isothermal region is caused by progressive MeOH consumption and carbon poisoning of the catalyst surface.

CO₂-selectivity even at reaction temperatures below 623 K (Figure 2, lower panel). Despite the virtually identical surface stoichiometry of PdZn 1:1 for both catalysts, the selectivity is markedly different. This is consistently explained by the influence of subsurface composition on the electronic and geometric structure of the topmost “active” PdZn layer.

The electronic differences between the multilayer and monolayer alloys are illustrated in Figure 3 in a number of XPS spectra acquired *in situ* during the MSR reaction (Pd3d, Zn3d and valence band regions). The Pd 3d level of the multilayer alloy exhibits its typical maximum at 335.8 eV, whereas the monolayer surface alloy has a characteristic peak maximum at 335.3 eV. The intensity increase from the multilayer to the monolayer Pd3d state is meaningful, too, because it reflects the higher detectable subsurface Pd fraction of the monolayer state while keeping the same 1:1 PdZn surface composition.

The valence band spectra reveal another significant difference. Whereas the multilayer alloy shows a “Cu-like” valence band, i.e. a significantly reduced density of states between ≈ 2.3 eV and 0 eV, the monolayer alloy, despite its 1:1 surface composition, rather resembles a modified Pd surface with an increased density of states close to the Fermi level, approaching the valence band spectrum of clean Pd. Moreover, the most important difference is evident from the Zn 3d spectra acquired under MSR reaction conditions (that is in the presence of H₂O). Whereas the multilayer alloy activates water by forming a Zn-OH species, resulting in the 10.25 eV shoulder in Fig. 3 (dashed-red peak fit, middle panel), this species is not present on the monolayer alloy under identical conditions (blue curve). Consequently, the monolayer alloy does not activate water and CH₂O formed from methanol is not converted to CO₂, but rather dehydrogenated toward CO. In analogy to the AES intensity curve of Fig. 1 (a), the integrated Zn3d intensity decreases considerably when switching from the multilayer to the monolayer alloy, again supporting the subsurface Zn-lean character of the remaining 1:1 PdZn surface alloy.

The Pd3d and valence band results were corroborated by the corresponding C1s spectra (supporting information S3). Signatures of CH₂O or related oxygenates were observed up to 505 K, i.e. for the multilayer alloy. Around 573 K and higher, the surface CH₂O was replaced by CO, pointing to the transformation of multilayer to monolayer alloy.

In summary, there is clear evidence that both the geometric and the electronic structures of the multilayer and monolayer alloys are significantly different. We have demonstrated that the CO₂-selective multilayer alloy features a lowered density of states close to the Fermi edge at surface ensembles of PdZn exhibiting a “Zn-up” corrugation, which represent the “bifunctional” active sites both for efficient water activation and for steering of methanol dehydrogenation toward H₂CO. The pronounced electronic and structural effects on the catalytic properties of the topmost active layer are driven by the composition of the

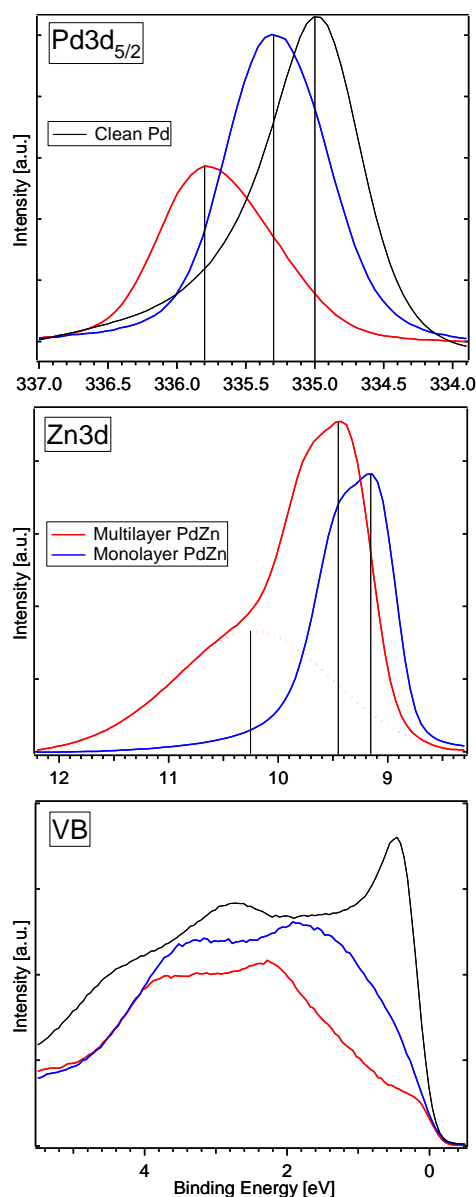


Fig. 3: HP-XPS spectra (Pd3d, Zn3d and valence band regions) acquired *in situ* during MSR on the PdZn 1:1 multilayer (red curves) and monolayer alloy (blue curves). For comparison, the respective clean Pd spectra are added (black lines). The oxidised ZnOH component is highlighted by the dashed red line (middle panel). Pd 3d and valence band regions were recorded with 650 eV photon energy, the Zn3d region at 120 eV in order to enhance the sensitivity for the surface-limited ZnOH. Reaction conditions: 0.12 mbar methanol, 0.24 mbar water, 553 K.

second (“subsurface”) layer, due to variations of the Zn-coordination of both Pd and Zn surface atoms.

Based on the current findings, likely intermediates for CO₂-selective MSR on the multilayer PdZn 1:1 alloy can be proposed (Scheme 1). While the central role of formaldehyde (which is formed by dehydrogenation of methanol via methoxy) is obvious from the present results, a key issue concerns the local structural and molecular chemistry responsible for selective CO₂ formation. Based on the analogy to Cu surfaces, Iwasa et al. suggested that CH₂O is

preferentially adsorbed in a $\eta^1(\text{O})$ -structure (bonding via oxygen, right side), whereas an $\eta^2(\text{C},\text{O})$ -structure (left side) prevails on metallic Pd and Pt [1]. Both types were observed by Jeroro et al. using HREELS [6] after formaldehyde adsorption in UHV at 150–200 K. DFT calculations favoured a η^2 top-bridge-top (tbt) configuration with the C and O atoms bridging two substrate atoms, and revealed significantly increased barriers for the undesired formaldehyde dehydrogenation to -CHO on PdZn and Cu, as compared to Pd [11,12]. The DFT-predicted stabilization of formaldehyde is clearly supported by the present experimental study. According to a related DFT study dedicated to a thermodynamic analysis of MSR surface species at ≈ 500 K and realistic reactant pressures [13], water is efficiently activated at PdZn surface ensembles on PdZn(111), as again corroborated by our study. The dominant oxygen-containing surface species on PdZn is OH_{ads} (at 3-fold hollow sites with a larger coordination of Zn atoms) rather than O_{ads} .

Open mechanistic questions are related to the elementary steps of reaction between coadsorbed formaldehyde and water species, finally leading to CO₂ and H₂ desorption. The nucleophilic addition of surface hydroxyls to adsorbed formaldehyde would result in a dioxomethylene species. The latter was proposed in several studies (Cu and PdZn related) as key intermediate of MSR or its microscopic reversal MeOH synthesis [14,15,16]. Dioxomethylene would then dehydrogenate to a formate group, and subsequent decarboxylation would finally result in CO₂ (gas) and associative desorption of H_{ads} . So far, it turned out difficult to verify this mechanistic picture spectroscopically on Cu-based catalysts [17], most likely due to the short lifetime of the key intermediates.

A final comment concerns differences between the MSR reaction on the planar PdZn surface alloys and on ZnO-supported PdZn nanoparticles. On the model catalysts, subsurface Zn depletion occurs via Zn dissolving in the Pd bulk, whereas this route is not available on the highly stable 1:1 nanoparticles. Also, alloying of Pd with metallic (deposited) Zn occurs at lower temperature than alloying of Pd with hydrogen-reduced ZnO. Additional promotion of water activation at PdZn bimetal – ZnO boundary sites or the partially reduced ZnO support itself (which also exhibits a rich catalytic chemistry) could be important for maximizing the conversion of formaldehyde to CO₂. Despite these differences, the complexity of technical Pd-ZnO catalysts prevents a detailed understanding of the molecular processes at the active site. Thus, studies of structure-selectivity relations on well-defined model systems are essential to unravel the elementary mechanisms at the atomic scale.

In summary, we demonstrated that this approach, combined with spectroscopic surface analysis under UHV and during reaction at realistic pressures, can be utilized to explain the different CO₂-selectivities of multilayer and monolayer PdZn surface alloys, despite their equal surface stoichiometry of 1:1. The subsurface layers steer the electronic and geometric structure of the topmost catalytically active layer (valence band density of states, corrugation) and are thus mainly responsible for the surface chemistry. Future studies will reveal whether this concept can be extended to oxide supported PdZn nanoparticles.

References

- [1] N. Iwasa, N. Takezawa, *Top. Catal.* 22 (2003) 215.
- [2] S. Penner, B. Jenewein, H. Gabasch, B. Klötzer, D. Wang, A. Knop-Gericke, R. Schlögl, K. Hayek, *J. Catal.* 241 (2006) 14.
- [3] A. Bayer, K. Flechtner, R. Denecke, H.-P. Steinrück, K. H. Neyman, N. Rösch, *Surf. Sci.* 600 (2005) 78.
- [4] H. Gabasch, S. Penner, B. Jenewein, B. Klötzer, A. Knop-Gericke, R. Schlögl, K. Hayek, *J. Phys. Chem. B* 110 (23) (2006) 11391.
- [5] G. Weirum, M. Kratzer, H.-P. Koch, A. Tamtögl, J. Killmann, I. Bako, A. Winkler, S. Surnev, F.P. Netzer, R. Schennach, *J. Phys. Chem. C* 113(22) (2009) 9788.
- [6] E. Jeroro, J.M. Vohs, *J. Am. Chem. Soc.* 130 (2008) 10199.
- [7] W. Stadlmayr, S. Penner, B. Klötzer, N. Memmel, *Surf. Sci.* 603(1) (2009) 251.
- [8] I. Bako, R. Schennach, G. Palinkas, *Journal of Physics: Conference Series* 100 (2008) 052067.
- [9] G. Rupprechter, *Advances in Catalysis* 51 (2007) 133.
- [10] T. Conant, A.M. Karim, V. Lebarbier, Y. Wang, F. Girgsdies, R. Schlögl, A. Datye, *J. Catal.* 257 (2008) 64.
- [11] K. Neyman, K.H. Lim, Z.-X. Chen, L.V. Moskaleva, A. Bayer, A. Reindl, D. Borgmann, R. Denecke, H.-P. Steinrück, N. Rösch, *PCCP* 9(27) (2007) 3470.
- [12] K. H. Lim, Z. X. Chen, K. M. Neyman, N. Rösch, *J. Phys. Chem. B*, 110 (2006) 14890.
- [13] K. H. Lim, L. Moskaleva, N. Rösch, *ChemPhysChem* 7 (2006) 1802.
- [14] Z.-M. Hu, H. Nakatsuji, *Chem. Phys. Lett.* 313(1,2) (1999) 14.
- [15] N. Takezawa, N. Iwasa, *Catal. Today* 36 (1997) 45.
- [16] K. Takahashi, N. Takezawa, H. Kobayashi, *Appl. Catal.* 2(6) (1982) 363.
- [17] B. Frank, F.C. Jentoft, H. Soerijanto, J. Kröhnert, R. Schlögl, R. Schomäcker, *J. Catal.* 246 (2007) 177.